Toxicology and Applied Pharmacology 361 (2018) 27–35

Contents lists available at ScienceDirect

Toxicology and Applied Pharmacology

journal homepage: www.elsevier.com/locate/taap

Dosimetry of inhaled elongate mineral particles in the respiratory tract: The impact of shape factor

Bahman Asgharian[a,*], T. Price Owen[b], Eileen D. Kuempel[c], Annie M. Jarabek[d]

[a] Applied Research Associates, Raleigh, NC, United States
[b] Applied Research Associates, Arlington, VA, United States
[c] National Institute for Occupational Safety and Health, Cincinnati, OH, United States
[d] U.S. Environmental Protection Agency, Research Triangle Park, NC, United States

ARTICLE INFO

Keywords:
Dosimetry modeling
High aspect ratio
Elongate mineral particles (EMPs)
Asbestos
Fibers
Nanotubes
Inhalation
Respiratory
Risk assessment

ABSTRACT

Inhalation exposure to some types of fibers (e.g., asbestos) is well known to be associated with respiratory diseases and conditions such as pleural plaques, fibrosis, asbestosis, lung cancer, and mesothelioma. In recent years, attention has expanded to other types of elongate mineral particles (EMPs) that may share similar geometry with asbestos fibers but which may differ in mineralogy. Inhalability, dimensions and orientation, and density are major determinants of the aerodynamic behavior for fibers and other EMPs; and the resultant internal dose is recognized as being the critical link between exposure and pathogenesis. Insufficient data are available to fully understand the role of specific physicochemical properties on the potential toxicity across various types of fiber materials. While additional information is required to assess the potential health hazards of EMPs, dosimetry models are currently available to estimate the initially deposited internal dose, which is an essential step in linking airborne exposures to potential health risks. Based on dosimetry model simulations, the inhalability and internal dose of EMPs were found to be greater than that of spherical particles having the same mass or volume. However, the complexity of the dependence of internal dose on EMPs dimensions prevented a straightforward formulation of the deposition-dimension (length or diameter) relationship. Because health outcome is generally related to internal dose, consideration of the factors that influence internal dose is important in assessing the potential health hazards of airborne EMPs.

1. Introduction

In this article, we provide an overview of a mechanistic model based on the multi-path particle dosimetry (MPPD) structure (ARA Inc., 2015). MPPD is a freely available dosimetry model for inhaled poorly-soluble particles and fibers which has been developed through a number of research collaborations, including with the U.S. EPA and NIOSH. MPPD has been used in various assessment applications to predict the dose of inhaled particles, including elongate mineral particles (EMPs), to the respiratory tract (e.g., Jarabek et al., 2005; NIOSH, 2013). The term “mineral fiber” has been frequently used by non-mineralogists to encompass thoracic-size (i.e., capable of entering the thoracic region) EMPs occurring either in an asbestiform habit (e.g., asbestos fibers) or in a non-asbestiform habit (e.g., as needle-like [acicular] or prismatic crystals), as well as EMPs that result from the crushing or fracturing of non-fibrous minerals (e.g., cleavage fragments) (NIOSH, 2011). EMPs are high aspect ratio particles, which are defined as having length:width ratio of at least 3:1. Other high aspect ratio particle shapes include tubes, belts, and whiskers; particle size can be nanoscale ($\leq$100 nm) or microscale ($>$ 100 nm) in diameter; and chemical composition can be carbonaceous or mineral. Dosimetry models are not currently available for other elongate shapes (e.g., rectangular cuboid); however, circular cross-section serves as an average of various shapes for dose estimation of other high aspect ratio particles.

Inhalation of fibers such as asbestos and some other mineral fibers have been recognized as a health hazard (Stephenson et al., 1999; Hughes and Weill, 1986; IARC, 1989; Lippmann, 2014; Manning et al., 2002; O'Reilly et al., 2007; Roach et al., 2002; Bibby et al., 2016; Feder et al., 2017) associated with several exposure-related lung diseases and

Abbreviations: β, fiber length to aspect ratio; BPM, breaths per minute; CFD, computational fluid dynamics; CNT, carbon nanotube; d_{ei}, equivalent impaction diameter; d_{ev}, volume equivalent diameter; d_f, minor diameter; EMP, elongate mineral particle; FRC, functional residual capacity; IF, inhaled fraction; RT, lower respiratory tract; MMAD, mass median aerodynamic diameter; MOA, mode of action; MPPD, multi-path particle dosimetry; PU, pulmonary; TB, tracheobronchial; URT, upper respiratory tract

* Corresponding author at: Applied Research Associates, 8537 Six Forks Road, Suite 600, Raleigh, NC 27615-6545, United States.
E-mail address: basgharian@ara.com (B. Asgharian).

https://doi.org/10.1016/j.taap.2018.05.001
Received 12 January 2018; Received in revised form 24 April 2018; Accepted 1 May 2018
Available online 05 May 2018
0041-008X/

conditions such as pleural plaques, asbestosis, bronchogenic and pulmonary carcinomas, and mesothelioma (IARC, 1977; IARC, 2002; IARC, 2012; NRC, 1984; Wagner et al., 1985; Suzuki and Kohyama, 1984). Features of asbestos fibers that determine inhalability and fate of airborne fibers include dimensions, density, and shape; these features and chemical composition, surface properties, and durability influence the fiber biopersistence and potential adverse health outcomes (Barrett et al., 1989; Harrington et al., 1975; Morgan et al., 1977). In addition, the shape and dimension of inhaled asbestos fibers, including straight-rod amphibole (amosite, crocidolite, tremolite, actinolite and anthophyllite) and curly serpentine (chrysotile) asbestos, have been suggested as key components in initiating disease (Jaurand, 1989; Smith et al., 1972; Stanton and Wrench, 1973; Stanton et al., 1977; Stayner et al., 2008; Donaldson et al., 2013). As evidence and understanding evolved about the relationship between the dimensions of asbestos fibers and their ability to cause nonmalignant respiratory disease and cancer, interest increased in the potential hazard of inhalation exposure to other EMPs.

The dimensions and density of fibers, including elongate mineral particles (EMPs) and other high-aspect ratio particles, affect the inhaled, deposited, and retained doses of these airborne materials (Asgharian and Anjilvel, 1998; NIOSH, 2011). Dosimetry models that describe these particle properties and biophysical kinetic processes provide the critical link between the airborne exposure and the internal dose at the target tissue sites for estimating the risk of adverse health effects. Exposure characteristics data that are needed as dosimetry model inputs (i.e., airborne concentration, and the number, surface area, or mass median diameter of an aerosol and its accompanying size distribution) are readily measured. While animal and cellular studies of fibers and other EMPs have shown adverse health effects and have provided insights on biological disease mechanisms (Yegles et al., 1995; Adamson 1997; Siegrist et al., 2014), there are uncertainties in translating the doses across various experimental systems in order to predict disease risk in humans (Jarabek et al., 2005; Kuempel et al., 2015). For example, in addition to exposure concentration and duration, retrospective dose reconstruction of epidemiological studies depend on the adequacy of both the exposure characterization, including size fraction or distribution and the type of sampling (e.g., either personal or area), and aspects of analytical characterization (e.g., counting rules employed to determine the sizing and limitations of imaging technologies).

To aid this translation, dosimetry models have been constructed to estimate internal dose given the exposure conditions and the properties of the airborne particles. For example, as illustrated in this paper, the inhalability and deposition fractions of spherical particles and EMPs in the respiratory tract regions depend on the particle shape, size, and other properties. Dosimetry models are simply mathematical descriptions of mechanisms and processes involved in inhalation, deposition, and retention of inhaled substances as a function of key parameters such as lung geometry and structure, lung volumes, breathing rates and parameters, and the physicochemical characteristics of the inhaled substances (e.g., EMPs). Uncertainty in estimating health risk and deriving exposure limits is reduced by using validated dosimetry models to estimate human-equivalent doses.

Dosimetry modeling can provide a translation framework for interspecies extrapolation, setting exposure limits to naturally occurring EMPs or to new man-made EMPs that may be produced, or for in vitro to in vivo (IVIVE) extrapolation of mechanistic assays. Application of dosimetry models thus aids translation of results and refines characterization of health risk by aligning and predicting the inhaled, deposited, or retained doses from a variety of exposure conditions.

In addition to inherent particle properties, the toxicity of EMPs depends on deposition in the respiratory tract due to aerodynamic behavior, and on retention due to shape and chemical properties. Determinants of aerodynamic behavior and biological responses to EMPs in the respiratory tract that are relevant for defining various internal dose metrics include the following: physicochemical properties, such as physical dimensions (length and width) and distribution, density, shape, and hygroscopicity which dictate inhalability and deposition; chemical composition, including factors such as solubility and surface ions which dictate clearance, retention and tissue response; and the exposure concentration in air. The density and geometry of an aerosol influences its aerodynamic behavior and resultant inhalable fraction (IF), deposition, and clearance in the respiratory tract (Yu et al., 1990a, 1990b, 1991; Sturm and Hofmann, 2009). For spherical particles, only one dimension (and its distribution) is needed to define its aerodynamic behavior, namely, radius or diameter of the particle. However, for straight-rod or needle-like shaped particles, there will be at least the two dimensions of length and diameter or multiple dimensions if the shape is more complex. Similarly, the joint size distribution has to be described for each dimension of elongated particles as compared with only one distribution of diameter or radius for spherical particles. Thus, mathematical description of EMPs is far more complicated than that of spherical particles, which calls for a separate treatment to account for the influence of dimensions on internal and retained doses and the subsequent health effects.

Consensus is evolving on the influence of dimensions or shape of inhaled EMPs and other high-aspect ratio particles on their resultant toxicity and health consequence. The diameter and length of EMPs influence deposition, clearance, and surface activity. While length has been suggested as the critical parameter dominating its behavior and health impact once entering the respiratory tract (e.g., Roggli, 2015), other dose metrics such as surface area and number of particles are being explored as potentially more mechanistically relevant. Criteria have been suggested for the toxicity of asbestos as a function of the fiber dimensions (Stanton et al., 1981; Pott, 1987; Lippmann, 1990; Berman et al., 1995; Quinn et al., 2000; reviewed in Stayner et al., 2008). However, these simplified criteria may not adequately account for the influence of the aerodynamic mechanisms discussed above in determining first inhaled and deposited dose, and then the retained dose, which depend on density and all dimensions of the EMPs or other high-aspect ratio particles. Other physicochemical properties such as solubility and surface reactivity can affect the clearance and retention of particles in the respiratory tract. When different types of particles are compared, inhaled dose are more appropriately expressed as particle volume, particle surface area, or number of particles rather than mass, depending on the mode of action for the toxic effect being evaluated (Oberdörster et al., 1994; Jarabek et al., 2005; Kuempel et al., 2015). Hence, relying on a single dimension as a predictor of the toxicity of EMPs would be inconsistent with the emerging understanding of the toxicokinetic and toxicodynamic mechanisms of inhaled particles. A dosimetry model enables the evaluation of different metrics of dose (e.g., particle mass, volume, surface area in specific respiratory tract regions) for interspecies dose-response extrapolation.

The MPPD model also helps to identify key parameters that control deposition and thus potential health impact. The three independent events of inhalability, deposition, and clearance – which control the internal dose and potential health impact – are briefly discussed below to shed light on the relationship between the dimensions of EMPs and potential for toxicity associated with the internal dose. Finally, we compare the deposition fractions of spherical and EMPs in the human respiratory tract based on simulated exposure scenarios using representative dimensions of airborne EMPs.

2. Inhalation dosimetry concepts

The respiratory tract is comprised of three major anatomical regions distinguished by their function and composition: the LRT includes the tracheobronchial (TB) and pulmonary (PU) regions, while the upper respiratory tract (URT) refers to the head airways (nasal and oral cavities). This section provides a brief overview of the factors influencing inhaled particle interaction with the anatomical and physiological features within those regions.

2.1. Overview of particle inhalation and fate

Three key events occur during an inhalation exposure, which depend on the density and dimensions of EMPs, and relate the estimated dose to health outcomes. First, during inhalation of EMPs, the inertia of inhaled EMPs may prevent transport of all airborne EMPs into the oral and nasal cavities. The inertial effects are different for spherical particles and EMPs and thus, so is their inhalability or inhaled fraction. Second, the transport and deposition of EMPs in the airways of the respiratory tract are directly related to their geometry (dimensions) and aerodynamic behavior (i.e., the particle geometry interacting with the airflow which is dictated by ventilation rate and anatomy). Volumetric flow is different in each major area of the respiratory tract with bulk flow dominating in the upper respiratory tract (URT) and the tracheobronchial (TB), and is also influenced by breathing mode (i.e., nasal or oral breathing). Impaction and interception dominate in these regions. Other external forces due to gravity, electrostatic charges, and diffusion also dictate the transport and deposition in the airways. These forces are different for EMPs and spherical particles and so will be their deposition pattern and amount deposited on airway surfaces. In addition, the net hydrodynamic viscous resistance force between the EMPs and air influences the position and orientation of EMPs in the airflow and thus transport and deposition. Consequently, the deposited dose of particles and EMPs are different even when particle mass and airborne concentration are the same. Finally, clearance of the deposited spherical particles and EMPs are different particularly in the lower respiratory tract (LRT). The retained dose in both the TB and PU regions is influenced by the shape and dimensions of deposited insoluble particles. For example, the increased dimensions (length and diameters) of EMPs may influence their dissolution rate or their ability to translocate into the interstitial space, and may also alter the capability of alveolar macrophages to engulf and remove EMPs from the lungs. These three independent events (inhalation, deposition and clearance) act collectively to formulate the fate of inhaled particles and EMPs and thus their potential health impact upon inhalation. Thus, more inclusive sizing criteria as a function of key parameters of EMPs characteristics are necessary to distinguish toxic versus non-toxic doses of EMPs and other high-aspect ratio particles (Vincent, 2005; Dement et al., 2015).

2.2. Inhalability

Inhalability of particles is defined as the fraction of EMP being inhaled, which depends on their ability to reach and enter the URT (Fig. 1). Inhalation creates a directed mass flow of airborne particles in the vicinity of facial region toward the nasal or oral openings. Particle momentum increases and reaches inhaled air velocity as they approach the URT. When approaching the URT, large particles with high inertia may not be able to follow the flow streamlines as they turn to enter the nasal airways. These particles are deposited on the neighboring surfaces such as the face and will escape entry to the respiratory tract. The fraction that overcomes the inertia and enter the URT is the inhaled fraction of particle. Correction for particle inhalability is required for accurate sampling and assessment of internal dose of airborne particles.

The majority of studies on particle inhalability under different environmental conditions (corresponding to high, low, and no wind speed) are conducted under controlled laboratory conditions and often with manikins in wind tunnels (Armbruster and Breuer, 1982; Hinds and Tatyan, 1998; Kennedy and Hinds, 2002; Ogden and Birkett, 1977; Vincent and Mark, 1982; Aitken et al., 1999; Breyess and Swift, 1990; Hsu and Swift, 1999). Modeling studies using computational fluid dynamics (CFD) have been performed to develop predictive models for particle inhalability (Anthony and Flynn, 2006). While there is an extensive database on the inhalability of (spherical) particles, there are no experimental or modeling studies on non-spherical particles and EMPs. Such studies are needed to refine extant particle and fiber models given the potential enhanced toxic effect of EMPs due to their shape. Distinct differences in geometry are expected to produce a significant difference in inhalability profile between particles and EMPs.

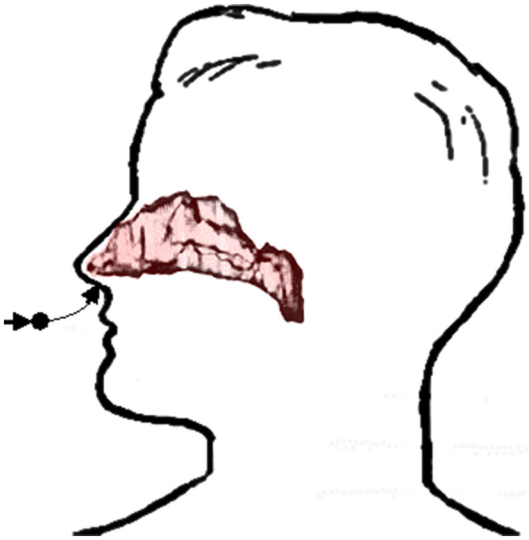

Fig. 1. Traveling path of a particle toward the head airways to enter or escape inhalability into the upper respiratory tract.

A hybrid approach is adopted to develop a model to predict the inhalability of EMPs. The database on particle inhalability as noted above was used to develop semi-empirical relationships between inhalability and parameters on which it depended. The majority of existing studies related inhalability to particle diameter. However, inhalability is better described in terms of particle inertia represented by the non-dimensional parameter Stokes number (the ratio of kinetic energy of particles to the work done on particles to bring them to a complete halt), which is the dominant parameter dictating entrance into the URT. To extend to EMPs, particle Stokes number was replaced by that for EMPs in the inhalability component of MPPD for spherical particles. Consequently, particle diameter was replaced with an equivalent impaction diameter (Yu et al., 1986) to obtain a semi-empirical relationship for inhalability as a function of its inertia. Equivalent diameter for each deposition mechanism (e.g., impaction) is the diameter of an equivalent sphere which results in the same amount of deposition as EMPs. The model was subsequently used to predict the inhaled fraction for different size EMPs and different breathing modes (nasal or oral) of inhalation.

Fig. 2 gives the inhaled fraction EMPs in humans and rats as a function of calculated equivalent impaction diameter (d_{ei}) using the MPPD model, v. 3.04 (ARA, Inc, 2015). Calculation of a d_{ei} relies on the premise that an equivalent sphere diameter is used to predict inhaled and deposited fractions of EMPs. At an equivalent impaction diameter, both spherical particles and EMPs would have the same inertia, which is represented by the Stokes number. Yu et al. (1986) derived expressions for impaction diameter by equating the Stokes number of particles and EMPs.

$$\frac{d_{ei}}{d_f} = \left(\frac{\rho}{\rho_0 \bar{C}}\right)^{1/2} \beta^{1.3} \tag{1}$$

where d_f is the EMP minor diameter, β is the EMP aspect ratio, $\bar{c}$ is the orientation effect, and ρ and ρ_0 are the EMP density and unit density, respectively. Predicted inhalation fractions (IFs) were in good agreement with reported measurements of impaction diameter (Burke and Esmen, 1978; Khan, 1982).

Predictions were based on ventilation rates associated with a light activity pattern, which was 20 m^3/d in humans and 0.62 m^3/d in rats and simulating calm wind conditions. The inhaled fractions in humans were calculated for oral and nasal breathing modes. Inhaled fraction

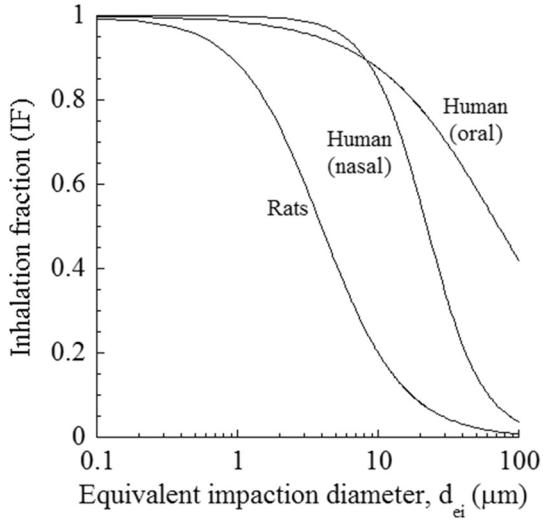

Fig. 2. Inhaled fraction in humans (20 m^3/day) and rats (0.62 m^3/day) versus a calculated fiber impaction equivalent diameter (d_{ei}). Oral or nasal breathing mode is simulated for humans whereas rats are obligate nasal breathers.

decreased with increasing EMP size. All EMPs were inhalable in humans for d_{ei} under 10 μm. Inhalability decreased for larger-diameter EMPs and more significantly for nasal breathing than for oral breathing. EMPs of length longer than 20 μm did not enter the nasal passages and were not inhaled, in contrast to oral breathing, where EMPs as long as 1 μm were still inhalable (inhaled fraction around 10%). Rats are obligate nasal breathers and thus the results in Fig. 1 represent nasal breathing for that species. Inhalability in rats was much lower than for humans because of smaller nasal geometry and significantly lower ventilation rates. EMPs as small as 0.1 μm in minor diameter were partially inhalable (about 98%). Inhalability drops much faster with increased particle size in rats than in humans. About 90% of EMPs are inhalable at d_{ei} of 1 μm but only about 10% at 10 μm d_{ei}. Lower number or mass of EMPs entering the respiratory tract of rats compared to that of humans, emphasizes the need for equivalent and not equal exposure scenarios to inflict similar biological outcomes. The difference in inhalability increases significantly for coarse aerosols. Thus, differences in inhalability in humans and rats must be taken into account in extrapolation of dose and response data from rodent inhalation studies to humans. Rat-to-human data extrapolation will be irrelevant regardless of exposure concentration when inhalability in rats drops to zero.

Inhaled fraction of a theoretical EMP aerosol was calculated and plotted against the minor diameter to examine the effect of shape and dimensions on inhalability. EMPs had volume-equivalent spherical diameters (d_{ev}) of 10 μm and 100 μm with different physical dimensions, which varied from a long and thin to short and thick until reaching spherical geometry (Fig. 3A). Using calm wind conditions, a typical tidal volume of 625 cm^3, a breathing frequency of 12 breaths per minute (BPM), and a functional residual capacity (FRC) of 3300 cm^3 via nasal breathing for the simulations, the predicted inhaled fraction of 100 μm d_{ev} EMPs was considerably lower than that of the 10 μm d_{ev} EMPs (Fig. 3B). Inhalability also decreased as the shape of EMPs changed, i.e., as they became shorter and thicker. Particle geometry was spherical when the diameter of EMPs was the same as the equivalent volume diameter (i.e., 10 μm and 100 μm). One notable conclusion from this result is that EMPs are more inhalable than spherical particles of the same volume or mass and hence more available in the respiratory tract for deposition. Thus, based on geometry alone, longer EMPs have a higher inhalability than shorter EMPs. However, only a fraction of all inhaled particles deposit in the respiratory tract, and it is the deposited dose of inhaled particles that is generally considered to be more closely associated with potential health outcomes.

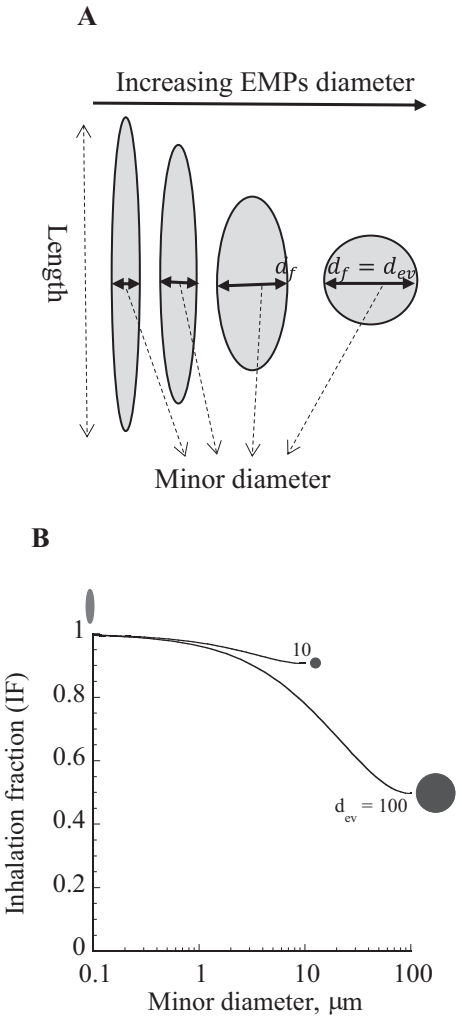

Fig. 3. A. Particle geometry for equivalent volume diameter (d_{ev}) of elongate mineral particles (EMPs). B. Predicted inhaled fraction (IF) for nasal breathing simulation of d_{ev} of 0.1, 10 and 100 μm in the human oral cavity as a function of the EMPs minor diameters. Particle shapes associated with these minor diameters are illustrated.

2.3. Particle transport and deposition

Transport and deposition of inhaled EMPs depend on their geometry (wall trapping) and aerodynamic properties. Several major deposition mechanisms influence the removal of airborne EMPs from the inhaled air, each corresponding to an external force and differ in relative contribution to deposition depending on the respiratory tract region as shown in Fig. 4. The main deposition mechanisms for inhaled particles and fibers include the following: interception, inertial impaction, gravitational settling, Brownian diffusion, and electrostatic charge. These mechanisms act collectively to cause a net deposition of particles throughout the respiratory tract in accordance with the regional significance of each deposition mechanism.

Interception is a significant mechanism for high-aspect ratio particles such as EMPs. Inertial impaction is the mechanism that causes partial entry of airborne particles into the head airways on inhalation. Due to their elongated geometry, EMPs also intercept the respiratory tract surfaces and deposit as they enter the LRT, at the main bronchial bifurcation, or on airway walls. When particles approach an airway bifurcation, the airflow splits and switches direction to exit through

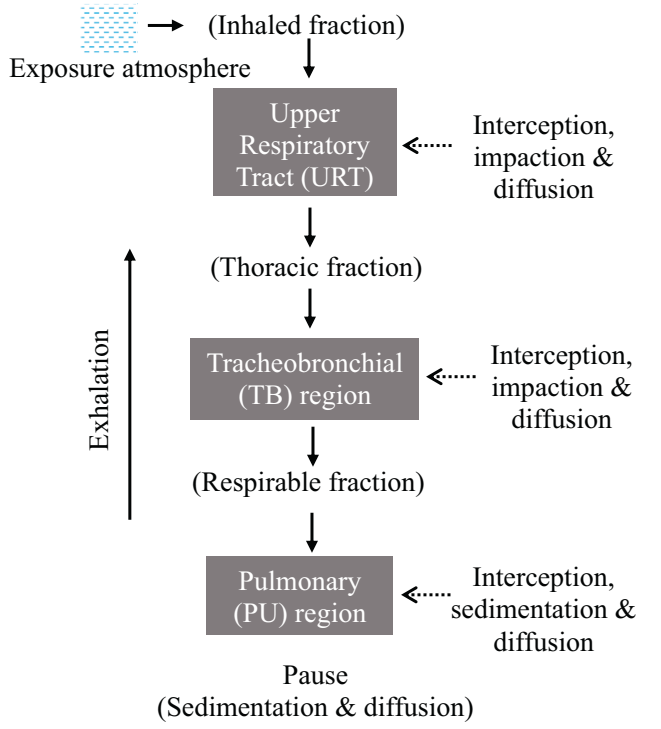

Fig. 4. The fate of inhaled particles through different regions of the respiratory tract based on mechanisms of transport and deposition.

daughter branches. Heavy particles will deviate from the flow streamlines (depending on the inertia) and may collide with the walls of the carina according to their inertia. The particle's mass influences its inertia (and since mass equals density times volume, the particle density and dimensions also play a role) – the higher the inertia, the higher the probability of deposition near the bifurcation region. Inertial impaction is significant for heavy particles when flow velocity is high (typically at the proximal region of the LRT). Gravitational settling is the result of deposition due to the force of gravity and is directly related to the mass of each individual EMPs. It is significant for particles with micrometer and larger diameters when the airflow rate in the lung has subsided in the distal portion of the LRT and there is an adequate time for particles to deposit by the force of gravity. Finally, EMPs may deposit via Brownian diffusion. Brownian diffusion is the random force on particles from collision with the surrounding air molecules. The collisions result in a net particle movement from regions of particle concentration (near the center of airways) to low concentration (at the walls). This deposition mechanism is significant for particles with sub-micrometer and smaller diameters in the deep lung where the airflow velocity is greatly diminished (i.e., at low Reynolds number defined as the ratio of inertial to viscous forces at less than unity). Particles that carry charge may deposit primarily by specific electrical forces called image forces and secondarily by space charges.

2.4. Particle retention

The retained dose of inhaled EMPs depends on the degree of biological clearance (mucociliary, alveolar macrophage-mediated) and physical dissolution in lung cells/fluids, which are influenced by their shape and dimensions. In the absence of mechanistic information (such as mucociliary velocity and macrophage movement), observations on particle movement from lung surfaces through tissues into the interstitium and lymph nodes were used to calculate compartment specific rate constants (ICRP, 1994) or develop empirical relationship for rate constants as a function of the mass (Yu et al., 1990a) and dimensions of the retained particles (Yu et al., 1990b). Modeling of the retained mass of EMPs should also account for their dimensions and longitudinal or traversal splitting, as derived previously for chrysotile asbestos based on available data of the mean length and diameter at consecutive post-exposure time intervals (Yu et al., 1991). Lack of mechanistic information limits the analysis of respiratory tract burden as a function of the dimensions of EMPs.

3. Dosimetry model components

The dosimetry model components and input parameters that allow prediction of the internal dose include the particle dimensions and density, the airway geometry and volumes, and the ventilation rate and breathing mode (e.g., either nasal, oral or oro-nasal). Transport modeling starts with identifying the characteristics of the inhaled aerosol, which include particle size dimensions (length and width), distribution, density, and exposure concentration. The size distribution is typically lognormal but can take on different distributions depending on generation or sampling method. Measurement information on the bivariate size distribution (length and diameter) of EMPs is necessary to accurately describe the aerodynamic behavior (Cheng, 1986). The bivariate size distribution data also provides the information needed to apply a simple method to convert the number concentration to surface area and mass concentration (Cheng, 1986).

A fraction of a given particle or fiber aerosol is unable to enter into the respiratory tract due to the high inertia of individual particles or fibers. As discussed in the Inhalability section, semi-empirical models under different environmental conditions are used to predict fractions that do and do not enter the URT. Flow in the URT is very high and mostly turbulent. Thus, the inhaled fraction of particles that are able to enter the URT deposit by inertial impaction for heavy particles and Brownian diffusion for light particles. Mathematical models are available for filtering efficiency of inhaled fraction in the URT region by different deposition mechanisms, which are used to predict the fraction of inhaled particles that deposit in this region and the fraction that enters the LRT (i.e., the thoracic fraction). Flow in the LRT decreases with distal depth into the lung due to flow splitting among different airways in each generation. However, it is still quite high in the tracheobronchial (TB) region. Particles in the TB region may also deposit by inertial impaction and Brownian diffusion for heavy and light particles. The lung volume increases exponentially in the PU region due to the presence of alveoli. Thus, the flow decreases rapidly (and the Reynolds number drops below one). Deposition in the PU region of particles within the thoracic fraction occurs by Brownian diffusion for light particles and gravitational settling for heavy particles. A pause follows inhalation, in which additional deposition by gravitational settling and Brownian diffusion occurs. Exhalation is the reverse of inhalation and follows a similar breathing pattern to that of inhalation. Particle deposition can also occur on exhalation.

The mathematical formulation for a mechanistic model such as the MPPD model of the transport and deposition of particles or fibers describes the above processes based on conservation of mass and momentum (Asgharian et al., 2001). The mathematical model includes the following four major components:

The first component is modeling the inhaled fraction and deposition in the URT based on either experimentally-based, derived semi-empirical relationships (e.g., Yu et al., 1980) or on CFD model predictions developed with reconstructed geometries of the URT from scan imagery (e.g., Schroeter et al., 2013).

The second component is a realistic description of the LRT geometry. The LRT geometry is structurally complex with thousands of conducting and millions of alveolated airways. The complexity makes comprehensive measurements of all airways impractical. Hence, single- and multiple-path lung geometries have been created from scan images of large airway and morphometry of small airways. The geometries include the major anatomical structure and features of the LRT for humans (Koblinger and Hofmann, 1985) and several laboratory animals

(e.g., Asgharian et al., 2014; Miller et al., 2014; Koblinger and Hofmann, 1988). The lung geometries are used for the model structure in which inhaled air distribution (lung ventilation) and particle and EMPs transport and deposition are calculated.

The third component of the transport model is a description of ventilation as it is responsible for the movement of particles in the respiratory tract. In principle, the transport (Navier-Stokes) equations have to be solved numerically by different computational schemes in all airways of the respiratory tract to obtain the flow distribution among different airways of the LRT. However, the task is formidable and infeasible because in-depth and thorough information on airway structure and dimensions are missing as mentioned above. In addition, there is no information on pleural pressure distribution, which is created by the weight of the LRT. The lack of information on geometry and outlet boundary conditions (pleural pressure information) currently reduces the enthusiasm for developing CFD models of the LRT, although imaging and computational techniques are rapidly advancing (Minard et al., 2012; Kuprat et al., 2013). Alternatively, the Navier-Stokes equations are linearized (at typical breathing rates) to allow independence of different sources of pressure drop in lung airways. Thus, the total pressure drop is determined by lung compliance, airway resistance, and flow inertance at high breathing rates. Flow inertance is due to the flow inertia (convection) that causes a pressure drop. Combined modeling and data measurements are used to develop models for pressure drop and lung airflow (ventilation) under varying breathing conditions to replace the flow momentum (Naiver-Stokes) equations.

Finally, a mathematical model such as the MPPD is based on species mass balance (component 4), which uses information from the first three components to predict deposition of particles throughout the entire respiratory tract. The model is mechanistic and based on first principles, which sets it apart from other semi-empirical models such as ICRP (1994) or NCRP (1997). The deposition of particles in any airway of the LRT by different mechanisms is the difference between inhaled and exhaled mass of particles plus the difference between initial and final mass of particles in the airway. Deposition is calculated in each generation of airways for the LRT and combined to find regional (URT, TB, and PU) and total (sum of regional) depositions.

4. Extension of MPPD to nonspherical particles

The behavior of EMPs aerosols and other high- aspect ratio particulate aerosols cannot be described by a single dimension such as physical diameter or aerodynamic diameter, as for spherical particles. The aerodynamic diameter of non-spherical particles (Timbrell, 1965) is defined as the diameter of a unit-density (1 g/cm^3) sphere that has the same settling velocity as that of a non-spherical particle. Given that the settling velocity is directly related to deposition by gravitational settling, this diameter can only be used for non-spherical particles if gravity is the only external force on particles in the respiratory tract. However, there are other forces (e.g., inertial impaction, interception, Brownian diffusion, and electrostatic charge) that could cause EMPs deposition in the respiratory tract as described earlier in this article. Hence, additional equivalent diameters are clearly needed. To be precise, there has to be one equivalent diameter for each deposition mechanism. The MPPD model v. 3.04 was recently extended to include non-spherical particles by replacing the particle diameter with the corresponding equivalent diameters (Kulkarni et al., 2011; Ku and Kulkarni, 2015) for each deposition mechanism in the corresponding deposition efficiency formula, as described earlier (Asgharian and Anjilvel, 1998; Asgharian and Yu, 1988, 1989).

4.1. Example of EMPs

In the following example, MPPD v. 3.04 was used to predict the deposition of EMPs in LRT airways as a function of dimensions and to compare with predictions for spherical particles. Regional deposition of a theoretical EMPs aerosol predicted to deposit in the LRT of humans is shown in Fig. 5 for a sitting activity level, including a typical tidal volume of 625 cm^3, breathing frequency of 12 breaths per minute (BPM), and functional residual capacity (FRC) of 3300 cm^3 via nasal breathing. Inhalability of EMPs was excluded to examine unbiased

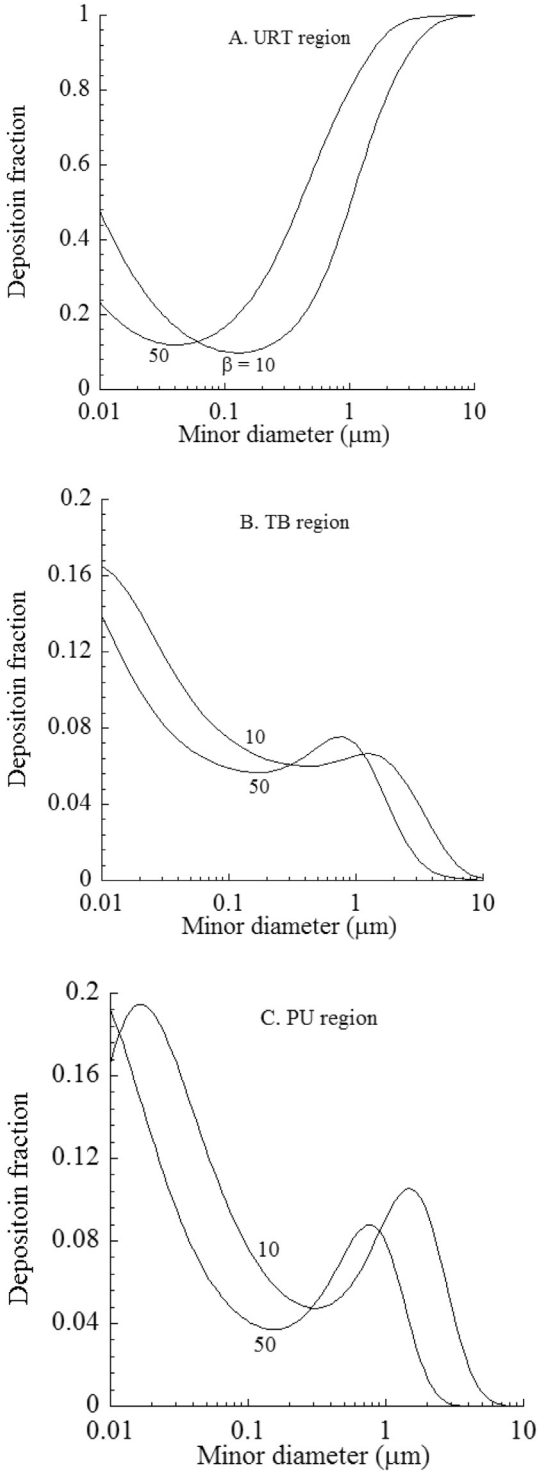

Fig. 5. Deposition fractions of inhaled elongate mineral particles (EMPs) in different regions of the human respiratory tract. Model simulations used a tidal volume of 625 cm^3, breathing frequency of 12 BPM, and an FRC of 3300 cm^3 via nasal breathing in no wind conditions. Inhalability of EMPs was not considered. Abbreviations: URT: upper respiratory tract; TB: tracheobronchial; PU: pulmonary; β: fiber aspect ratio (length/width); d_f: minor diameter.

deposition mechanisms in the LRT. Model predictions were made for deposition fraction plotted against EMPs diameter (d_f) and for EMPs length to diameter ratios (aspect ratio, β) of 10 and 50 in the URT (Fig. 5A), TB (Fig. 5B) and PU (Fig. 5C) regions. Deposition in the URT was by Brownian diffusion for light EMPs and inertial impaction for heavy EMPs, respectively. As seen, the deposition pattern was bell shaped. Deposition in the TB regions was also by inertial impaction and Brownian diffusion. However, filtering of EMPs by the URT affected the shape of the deposition curve in the TB region. Deposition in the PU was due to Brownian diffusion and sedimentation. However, the expected bell shape trend was further disrupted by the filtering of EMPs in the URT and TB regions. Particle filtering and cumulative effects of different deposition mechanism did not allow drawing a simple relationship between EMPs dimensions (e.g., diameter and aspect ratio) and deposition fraction in the different regions of the respiratory tract. The filtering effects were evident by the peak deposition around EMPs minor diameter of 1 μm in the TB region from URT (Fig. 5B) and peaks in the PU region around 0.01 μm and 1 μm due to EMPs deposition in the URT and TB regions. In addition, lower deposition of heavier of ultrafine EMPs were due to the filtering effects.

Comparison of EMPs deposition with that of spherical particles to evaluate the influence of EMPs dimensions on deposition in the respiratory tract were made in Fig. 6A. Deposition fractions were calculated assuming no deposition in the URT (Fig. 6B), which was a hypothetical scenario, and with deposition in the URT (Fig. 6C) to study the influence of URT filtering on subsequent LRT deposition. Three cases were studied: spherical particles of 1 μm diameter and two different EMPs, each of equivalent mass but with different aspect ratios of 10 and 50. Particle minor diameters were: 1 μm (spherical), 0.33 μm (fiber with β = 10), and 0.2 μm (fiber with β = 50). Predicted deposition fractions in the TB and PU regions are given in Fig. 6B and C for the same breathing frequency (12 BPM) and tidal volume (625 cm^3) as in Fig. 5. Deposition in the LRT increased when URT deposition was excluded, and may occur with an oral breathing mode. With URT filtering, there was a smaller fraction of longer and thinner EMPs in the TB and PU regions compared to that for shorter and thicker EMPs. Deposition in the TB region was higher than that in the PU region for EPMs. In addition, deposition in the TB region increased with increasing EMP length, whereas PU deposition showed the reverse trend, partly due to the filtering by the TB region. There was not a clear pattern for TB deposition with EMP dimensions. Spherical particles deposited more in the LRT. Findings from Figs. 5 and 6 emphasizes the need for comprehensive dosimetry analyses using models over consideration of singular dimensions or aspect ratio alone to study the fate of inhaled fibers and EMP.

The findings from this example of EMPs deposition in the human respiratory tract in MPPD (v. 3.04) are compared to those in another model of a different type of elongated particles, carbon nanotubes (CNTs) (Sturm, 2015). In that model, single-walled CNTs were assumed to have a diameter of 5 nm and aspect ratios of 10, 100, or 1000. Multi-walled CNTs were assumed to have a diameter of 50 nm and the same aspect ratios as for SWCNT. Agglomeration of CNTs was not modeled. Particle density was assumed to be < 2.2 (density of graphite) since CNTs are not solid cylinders but form rolled sheets of carbon. Similar respiratory parameters for sitting (nasal breathing) conditions were used in Sturm (2015) and here, that is: tidal volume of 750 ml (vs. 625 ml here); 4.2 s/breaths (or 14.3 BPM) (vs. 12 BPM here); and FRC of 3300 ml in both studies. Predicted pulmonary (acinar) deposition of CNTs in sitting adults were ~10–25% in Sturm (2015), Figs. 4d and 6d) and ~8–10% for EMPs in this study (Fig. 6c of this article). Deposition of spherical particles (volume-equivalent diameter to the carbon nanotubes) in the pulmonary region was ~5–20% (Sturm, 2015, Fig. 6d), compared to ~10% for spherical particles with equivalent volume to EMPs (Fig. 6c of this article). Tracheobronchial deposition of spherical particles was ~2–7% in Sturm (2015), Fig. 6c and ~7% for EMPs (Fig. 6c in this article). Tracheobronchial deposition of CNTs was ~4–20% in Sturm (2015), Fig. 6c and ~5% for EMPs (Fig. 6c here). Despite the differences in the dimensions of elongated particles and the different dosimetry models used in these two analyses (Sturm, 2015 and

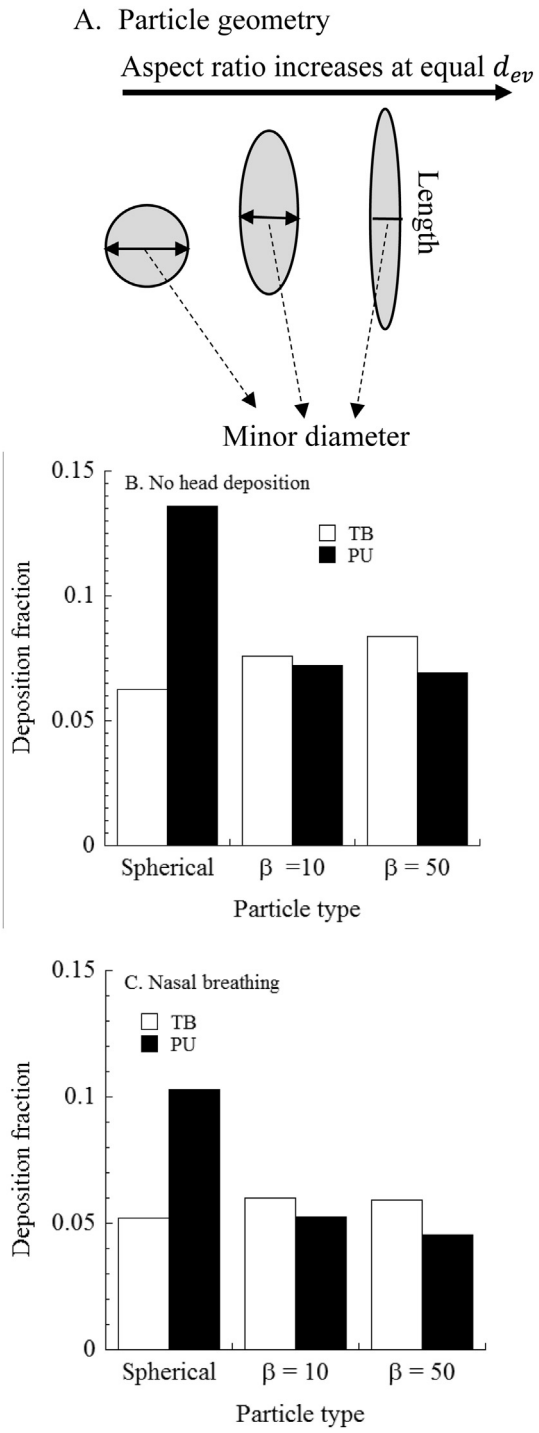

Fig. 6. Comparison of regional deposition fraction of spherical (equivalent volume diameter) particles and inhaled elongate mineral particles (EMPs) in the tracheobronchial (TB) and pulmonary (PU) regions of the human respiratory tract. A. Particle geometry for equivalent volume diameter (d_{ev}) of elongate mineral particles (EMPs); B. Predicted deposition fraction for simulation with no URT deposition; C. Predicted deposition fraction for simulation with nasal breathing. Spherical particles have diameter resulting in equivalent volume (d_{ev}) to fibers with the aspect ratio (length/width) (β) as indicated. Particle minor diameters are: 1 μm (spherical), 0.33 μm (fiber with β = 10), and 0.2 μm (fiber with β = 50). Simulation conditions were the same as in Fig. 5.

here), the estimated deposition fractions are similar. In this article, TB deposition fractions of EMPs were higher and PU deposition fractions were lower than those of volume-equivalent spherical particles (Fig. 6B and C). In contrast, Sturm (2015) reported increased TB and PU deposition fractions of the CNTs compared to volume-equivalent spheres at nasal breathing (Fig. 6C in Sturm, 2015). The purpose of this comparison was to provide a general evaluation of these EMPs modeling results compared to another model under similar conditions. Contradictory differences in LRT predictions are likely due to differences in filtering efficiencies of the nasal passages. Thus, the dimensions of inhaled particles including EMPs are shown to influence the estimates of the total and regional deposited doses in the human respiratory tract.

5. Conclusions

Dosimetry models account for critical determinants of deposition and clearance to predict the internal dose of inhaled particles including EMPs. These models are especially useful when substance-specific data are lacking and experimentation is infeasible. By providing mathematical descriptions of physical and physiological mechanisms that govern transport and deposition in airways of the respiratory tract, dosimetry models are able to predict the internal dose as a function of lung and breathing parameters and EMPs physical characteristics. Model predictions showed that due to the elongated geometry of EMPs, inhalability into the URT and deposition on lung airway surfaces is higher than for spherical particles. Dosimetry models provide a valuable tool for risk assessors, government agencies, stakeholders, and the scientific community in evaluating the potential health impact of inhaled particles and providing guidance on exposure limits.

Acknowledgements

The authors appreciate the technical reviews provided by Drs. James Brown, Bon-Ki Ku, Pramod Kulkarni, John Stanek, and Lisa M. Sweeney.

Funding

This study was funded in part by EPA Contract #EP-W-10-051 and NIOSH214-2011-M-38457 to Applied Research Associates, Inc.

Disclaimer

The findings and conclusions in this article are those of the authors and do not necessarily represent the views or policies of the U.S. Environmental Protection Agency (U.S. EPA) or the National Institute for Occupational Safety and Health (NIOSH). This article is not subject to U.S. copyright law.

References

Adamson, I.Y.R., 1997. Early Mesothelial Cell Proliferation after Asbestos Exposure: In Vivo and in Vitro Studies. Environmental Health Perspectives 5, 1205–1208.
Aitken, R.J., Baldwin, P.E.J., Beaumont, G.C., Kenny, L.C., Maynard, A.D., 1999. Aerosol inhalability in low air movement environment. J. Aerosol Sci. 30, 613–626.
Anthony, T.R., Flynn, M.R., 2006. Computational fluid dynamics investigation of particle inhalability. J. Aerosol Sci. 37, 750–756.
ARA, Inc, 2015. Multiple-path Particle Dosimetry Model (MPPD v. 3.04). Applied Research Associates, Inc., Raleigh, NC Available at: https://www.ara.com/products/multiple-path-particle-dosimetry-model-mppd-v-304.
Armbruster, L., Breuer, H., 1982. Investigation into defining inhalability. Ann. Occup. Hyg. 26, 21–32.
Asgharian, B., Anjilvel, S., 1998. A multiple-path model of fiber deposition in the rat lung. Toxicol. Sci. 44, 80–86.
Asgharian, B., Yu, C.P., 1988. Deposition of inhaled fibrous particles in the human lung. J. Aerosol. Med. 1, 37–50.
Asgharian, B., Yu, C.P., 1989. Deposition of fibers in the rat lung. J. Aerosol Sci. 20, 355–366.
Asgharian, B., Hofmann, W., Bergmann, R., 2001. Particle deposition in a multiple-path model of human lung. Aerosol Sci. Technol. 34, 332–339.
Asgharian, B., Price, O.T., Oldham, M., Chen, L.C., Saunders, E.L., Gordon, T., Mikheev, V.B., Minard, K.R., Teeguarden, J.G., 2014. Computational modeling of nanoscale and microscale particle deposition, retention and dosimetry in the mouse respiratory tract. Inhal. Toxicol. 26, 829–842.
Barrett, J.C., Lamb, P.W., Wiseman, R.W., 1989. Multiple mechanisms for the carcinogenic effects of asbestos and other mineral fibers. Environ. Health Perspect. 81, 81–89.
Berman, D.W., Crump, K.S., Chatfield, E.J., Davis, J.M., Jones, A.D., 1995. The sizes, shapes, and mineralogy of asbestos structures that induce lung tumors or mesothelioma in AF/HAN rats following inhalation. Risk Anal. 15, 181–195 (Correction in Risk Anal. 1995, 15(4), 541).
Bibby, A.C., Tsim, S., Kanellakis, N., Ball, H., Talbot, D.C., Blyth, K.G., Maskell, N.A., Psallidas, I., 2016. Malignant pleural mesothelioma: an update on investigation, diagnosis and treatment. Eur. Respir. Rev. 25 (142), 472–486. Dec. https://doi.org/10.1183/16000617.0063-2016 Review. PubMed PMID: 27903668.
Breyess, P.N., Swift, D.L., 1990. Inhalability of large particles into human nasal passages: in vivo studies in still air. Aerosol Sci. Technol. 13, 459–464.
Burke, W.A., Esmen, N., 1978. The inertial behavior of fibers. Am. Ind. Hyg. Assoc. J. 39, 400–405.
Cheng, Y.-S., 1986. Bivariate lognormal distribution for characterizing asbestos Fiber aerosols. Aerosol Sci. Technol. 53, 359–368. http://dx.doi.org/10.1080/02786828608959100.
Dement, J.M., Kuempel, E.D., Zumwalde, R.D., Ristich, A.M., Fernback, J.E., Smith, R.J., 2015. Airborne fiber size characterization in exposure estimation: evaluation of a modified transmission electron microscopy protocol for asbestos and potential use for carbon nanotubes and nanofibers. Am. J. Ind. Med. 58, 494–508. http://dx.doi.org/10.1002/ajim.22422.
Donaldson, K., Poland, C.A., Murphy, F.A., MacFarlane, M., Chernova, T., Schinwald, A., 2013. Pulmonary toxicity of carbon nanotubes and asbestos – similarities and differences. Adv. Drug Deliv. Rev. 65, 2078–2086.
Feder, I.S., Tischoff, I., Theile, A., Schmitz, I., Merget, R., Tannapfel, A., 2017. The asbestos fiber burden in human lungs: new insights into the chrysotile debate. Eur. Respir. J. 49, 1602534. http://dx.doi.org/10.1183/13993003.02534-2016.
Harrington, J.S., Allison, A.C., Badami, D.V., 1975. Mineral fibers: chemical, physicochemical and biological properties. Adv. Pharmacol. Chemother. 12, 291–402.
Hinds, W.C., Tatyan, K., 1998. Inhalability of large particles from mouth and nose breathing. J. Aerosol Sci. 29 (Suppl. 1), S277–S278.
Hsu, D.-J., Swift, W.C., 1999. The measurements of human inhalability of ultralarge aerosols in calm air using manikins. J. Aerosol Sci. 30, 1331–1343.
Hughes, J.M., Weill, H., 1986. Asbestos exposure – a critical review. Am. Rev. Respir. Dis. 33, 5–13.
IARC, 1977. IARC Monographs on the Evaluation of Carcinogenic Risk of Chemicals to Man: Asbestos. vol. 14 World Health Organization, International Agency for Research on Cancer, Lyon, France Available at: http://monographs.iarc.fr/ENG/Monographs/vol1-42/mono14.pdf.
IARC, 1989. In: Bignon, J., Peto, J., Saracci, R. (Eds.), Non-occupational Exposure to Mineral Fibres. IARC Scientific Publications No. 90. World Health Organization, International Agency for Research on Cancer, Lyon, France Available at: http://www.iarc.fr/en/publications/pdfs-online/sp90/.
IARC, 2002. IARC Monographs on the Evaluation of Carcinogenic Risks to Humans: Man-made Vitreous Fibres. vol. 81 World Health Organization, International Agency for Research on Cancer, Lyon, France Available at: http://monographs.iarc.fr/ENG/Monographs/vol81/mono81.pdf.
IARC, 2012. IARC Monographs on the Evaluation of Carcinogenic Risks to Humans: Arsenic, Metals, Fibres, and Dusts. A Review of Human Carcinogens, vol. 100C World Health Organization, International Agency for Research on Cancer, Lyon, France Available at: http://monographs.iarc.fr/ENG/Monographs/vol100C/mono100C.pdf.
ICRP, 1994. Human Respiratory Tract Model for Radiological Protection. Publication 66. International Commission on Radiological Protection. 24. Pergamon Press, Oxford, United Kingdom, pp. 272 Annals of ICRP.
Jarabek, A.M., Asgharian, B., Miller, F.J., 2005. Dosimetric adjustments for interspecies extrapolation of inhaled poorly soluble particles (PSP). Inhal. Toxicol. 17, 317–334. http://dx.doi.org/10.1080/08958370590929394.
Jaurand, M.C., 1989. A particulate state carcinogenesis: a survey of recent data on the mechanisms of action of fibres. IARC Sci. Publ. 54–73.
Kennedy, N.J., Hinds, W.C., 2002. Inhalability of large solid particles. J. Aerosol Sci. 33, 237–255.
Khan, R.A., 1982. A Method for Investigating the Deposition of Fibers and Spheres at the Carina in Excised Lungs. Ph.D. thesis. University of Pittsburgh.
Koblinger, L., Hofmann, W., 1985. Analysis of human lung morphometric data for stochastic aerosol deposition calculations. Phys. Med. Biol. 30, 541–556.
Koblinger, L., Hofmann, W., 1988. Stochastic morphological model of the rat lung. Anat. Rec. 221, 539–553.
Kuempel, E.D., Sweeney, L.M., Morris, J.B., Jarabek, A.M., 2015. Advances in inhalation dosimetry models and methods for occupational risk assessment and exposure limit derivation. J. Occup. Environ. Hyg. 12 (Suppl. 1), S18–S40. http://dx.doi.org/10.1080/15459624.2015.1060328.
Kulkarni, P., 2015. Measurement of transport properties of aerosolized nanomaterials. J. Aerosol Sci. 90, 169–181.
Kulkarni, P., Baron, P.A., Willeke, K., 2011. Aerosol, Measurement: Principles, Techniques, and Applications, 3rd edition. John Wiley & Sons, Inc., Hoboken, New Jersey.
Kuprat, A.P., Kabilan, S., Carson, J.P., Corley, R.A., Einstein, D.R., 2013. A bidirectional coupling procedure applied to multiscale respiratory modeling. J. Comput. Phys. 244 (Jul). http://dx.doi.org/10.1016/j.jcp.2012.10.021.
Lippmann, M., 1990. Effects of fiber characteristics on lung deposition, retention, and

disease. Environ. Health Perspect. 88, 311–317.
Lippmann, M., 2014. Toxicological and epidemiological studies on effects of airborne fibers: coherence and public health implications. Crit. Rev. Toxicol. 44, 643–695.
Manning, C.B., Vallyathan, V., Mossman, B.T., 2002. Diseases caused by asbestos: mechanisms of injury and disease development. Int. Immunopharmacol. 2, 191–200.
Miller, F.J., Asgharian, B., Schroeter, J.D., Price, O.P., Corley, R.A., Einstein, D.R., Jacob, R.E., Cox, T.C., Kabilan, S., Bentley, T., 2014. Respiratory tract lung geometry and dosimetry model for male Sprague-Dawley rats. Inhal. Toxicol. 26, 524–544.
Minard, K.R., Kuprat, A.P., Kabilan, S., Jacob, R.E., Einstein, D.R., Carson, J.P., Corley, R.A., 2012. Phase-contrast MRI and CFD modeling of apparent 3He gas flow in rat pulmonary airways. J. Magn. Reson. 221 (Aug), 129–138. http://dx.doi.org/10.1016/j.jmr.2012.05.007. (Epub 2012 May 23).
Morgan, A., Davies, P., Wagner, J.C., Berry, G., Holmes, A., 1977. The biological effects of magnesium-leached chrysotile asbestos. Br. J. Exp. Pathol. 58, 465–473.
NCRP, 1997. Deposition, retention and dosimetry of inhaled radioactive substances. In: National Council on Radiological Protection and Measurements, Bethesda, Maryland. Report 125.
NIOSH, 2011. Current Intelligence Bulletin 62: Asbestos Fibers and Other Elongate Mineral Particles: State of the Science and Roadmap for Research, Revised edition. DHHS (NIOSH) Publication No. 2011–159 U.S. Department of Health and Human Services, Public Health Service, Centers for Disease Control and Prevention, National Institute for Occupational Safety and Health, Cincinnati, Ohio Available at: https://www.cdc.gov/niosh/docs/2011-159/pdfs/2011-159.pdf.
NIOSH, 2013. Current Intelligence Bulletin 65: Occupational Exposure to Carbon Nanotubes and Nanofibers. DHHS (NIOSH) Publication No. 2013-145 U.S. Department of Health and Human Services, Public Health Service, Centers for Disease Control and Prevention, National Institute for Occupational Safety and Health, Cincinnati, Ohio Available at: https://www.cdc.gov/niosh/docs/2013-145/pdfs/2013-145.pdf.
NRC, 1984. Asbestiform Fibers: Nonoccupational Health Risks. National Research Council, National Academy Press, Washington, D.C.
Oberdörster, G., Ferin, J., Lehnert, B.E., 1994. Correlation between particle size, in vivo particle persistence, and lung injury. Environ. Health Perspect. 102 (Suppl. 5), 173–179.
Ogden, T.L., Birkett, J.L., 1977. The human head as a dust sampler. In: Walton, W.H. (Ed.), Inhaled Particles IV. Pergamon Press, Oxford, pp. 93–105.
O'Reilly, K.M.A., Mclaughlin, A.M., St. Willbeckett, W.S., Sime, P.J., 2007. Asbestos-Related Lung Disease. Downloaded from the American Family Physician Web site at www.aafp.org/afp. vol. 75.
Pott, F., 1987. Fiber as a carcinogenic agent [in German]. Zentralbl Bakteriol Mikrobiol Hyg. [B] 184 (1), 1–23.
Quinn, M.M., Smith, T.J., Eisen, E.A., Wegman, D.H., Ellenbecker, M.J., 2000. Implication of different fiber measures for epidemiologic studies of man-made vitreous fibers. Am. J. Ind. Med. 38 (2), 132–139.
Roach, H.D., Davies, G.J., Attanoos, R., Crane, M., Adams, H., Phillips, S., 2002. Asbestos: When the Dust Settles—An Imaging Review of Asbestos-Related Disease. http://dx.doi.org/10.1148/radiographics.22.suppl_1.g02oc10s167.
Roggli, V., 2015. The so called short fiber controversy. Arch. Pathol. Lab. Med. 39, 1052–1057.
Siegrist, K.J., Reynolds, S.H., Kashon, M.L., Lowry, D.T., Dong, C., Hubbs, A.F., Young, S.-H., Salisbury, J.L., Porter, D.W., Benkovic, S.A., McCawley, M., Keane, M.J., Mastovich, J.T., Bunker, K.L., Cena, L.G., Sparrow, M.C., Sturgeon, J.L., Dinu, C.Z., Sargent, L.M., 2014. Genotoxicity of multi-walled carbon nanotubes at occupationally relevant doses. Particle and Fibre Toxicology 11, 6. http://dx.doi.org/10.1186/1743-8977-11-6.
Schroeter, J.D., Asgharian, B., Price, O.T., McClellan, G.E., 2013. Computational fluid dynamics simulations of inhaled nano- and microparticle deposition in the rhesus monkey nasal passages. Inhal. Toxicol. 25, 691–701.
Smith, W.E., Hubert, D.D., Badollet, M.S., 1972. Biologic differences in response to long and short asbestos fibers. Ind. Hyg. Assoc. J. 33, 67.
Stanton, M.F., Wrench, C., 1973. Mechanisms of mesothelioma induction with asbestos and fibrous glass. J. Natl. Cancer Inst. 48, 797–821.
Stanton, M.F., Layard, M., Tegeris, A., Miller, E., May, M., Kent, E., 1977. Carcinogenicity of fibrous glass: pleural response in the rat in relation to fiber dimension. J. Natl. Cancer Inst. 58, 587–603.
Stanton, M.F., Layard, M., Tegeris, A., Miller, E., May, M., Morgan, E., Smith, A., 1981. Relation of particle dimension to carcinogenicity in amphibole asbestoses and other fibrous minerals. J. Natl. Cancer Inst. 67 (5), 965–975.
Stayner, L., Kuempel, E., Gilbert, S., Hein, M., Dement, J., 2008. An epidemiological study of the role of chrysotile asbestos fibre dimensions in determining respiratory disease risk in exposed workers. Occup. Environ. Med. 65 (9), 613–619.
Stephenson, D.J., Fairchild, C.I., Buchan, R.M., Dakins, M.E., 1999. A fiber characterization of the natural zeolite, mordenite: a potential inhalation health hazard. J. Aerosol. Sci. Technol. 30, 467–476.
Sturm, R., 2015. Nanotubes in the human respiratory tract - deposition modeling. Z. Med. Phys. 25, 135–145.
Sturm, R., Hofmann, W., 2009. A theoretical approach to the deposition and clearance of fibers with various size in the human respiratory tract. J. Hazard. Mater. 170, 210–218.
Suzuki, Y., Kohyama, N., 1984. Malignant mesothelioma induced by asbestos and zeolite in the mouse peritoneal cavity. Environ. Res. 35, 277–292.
Timbrell, V., 1965. Human exposure to asbestos: dust controls and standards. The inhalation of fibrous dusts. Ann. N. Y. Acad. Sci. 132, 255–273.
Vincent, J.H., 2005. Health-related aerosol measurement: a review of existing sampling criteria and proposals for new ones. J. Environ. Monit. 7, 1037–1053.
Vincent, J.H., Mark, D., 1982. Application of blunt sampler theory to the definition and measurement of inhalable dust. Ann. Occup. Hyg. 26, 3–19.
Wagner, J.C., Skidmore, J.W., Hill, R.J., Griffiths, D.M., 1985. Erionite exposure and mesotheliomas in rats. Br. J. Cancer 51, 727–730.
Yegles, M., Janson, X., Hang, Y.D., Renier, 1995. Role of fibre characteristics on cytotoxicity and induction of anaphase/telophase aberrations in rat pleural mesothelial cells in vitro: correlations with in vivo animal findings. Carcinogenesis 16, 2751–2785.
Yu, C.P., Diu, C.K., Soong, T.T., 1980. Statistical analysis of aerosol deposition in nose and mouth. American Industrial Hygiene Association Journal 42, 726–733.
Yu, C.P., Asgharian, B., Yen, B.M., 1986. Impaction and sedimentation deposition of fibers in airways. Am. Ind. Hyg. Assoc. J. 47, 72–77.
Yu, C.P., Asgharian, B., Chen, Y.K., 1990a. Deposition and clearance modeling of fibrous dusts in the lung. J. Aerosol Sci. 21, 308–371.
Yu, C.P., Asgharian, B., Abraham, J.L., 1990b. A mathematical model of alveolar clearance of fibers from the rat lung. J. Aerosol Sci. 21, 587–594.
Yu, C.P., Asgharian, B., Pinkerton, K.E., 1991. Intrapulmonary deposition and retention modeling of chrysotile asbestos fibers in rats. J. Aerosol Sci. 22, 757–763.